

# High-Resolution, Low-Delay, and Error-Resilient Medical Ultrasound Video Communication Using H.264/AVC Over Mobile WiMAX Networks

Andreas Panayides, Zinonas C. Antoniou, Yiannos Mylonas, Marios S. Pattichis, Andreas Pitsillides, and Constantinos S. Pattichis

**Abstract**—In this study, we describe an effective video communication framework for the wireless transmission of H.264/AVC medical ultrasound video over mobile WiMAX networks. Medical ultrasound video is encoded using diagnostically driven, error resilient encoding, where quantization levels are varied as a function of the diagnostic significance of each image region. We demonstrate how our proposed system allows for the transmission of high-resolution clinical video that is encoded at the clinical acquisition resolution and can then be decoded with low delay. To validate performance, we perform OPNET simulations of mobile WiMAX medium access control and physical layers characteristics that include service prioritization classes, different modulation and coding schemes, fading channel's conditions, and mobility. We encode the medical ultrasound videos at the 4CIF (704×576) resolution that can accommodate clinical acquisition that is typically performed at lower resolutions. Video quality assessment is based on both clinical (subjective) and objective evaluations.

**Index Terms**—Diagnostic region of interest (ROI), e-health, error resilience, flexible macroblock ordering (FMO), 4G, H.264/AVC, HSPA, m-health, mobile WiMAX, telemedicine, ultrasound video, video quality assessment (VQA).

## I. INTRODUCTION

CONTINUOUS advances in medical video coding, together with wider availability of current and emerging wireless network infrastructure, provide the key technologies that are needed to support m-health video communication technologies in standard clinical practice. Over the past decade, demand for mobile health systems has been growing [1]–[3]. Demand is driven by the need for responsive emergency telematics, remote diagnosis and care, medical education, as well as for mass pop-

ulation screening and emergency crisis management. Advancements in mobile health systems are expected to bring greater socioeconomic benefits, improving the quality of life of patients with mobility problems, the elderly, and people residing in remote areas, by enhancing their access to specialized care. Moreover, they will provide a critical time advantage that can prove life saving in life-threatening emergency incidents.

Current research in m-health video communications systems include modality-aware (m-aware) diagnostically driven systems, which adapt to the underlying wireless transmission medium [3]. Diagnostically driven systems often rely on the use of diagnostic regions of interest (ROIs) [4]–[6]. Adaptation to the wireless network's characteristics includes diagnostically relevant selection of the source encoding parameters and error control for addressing inevitable transmission errors. Clinical video quality assessment (VQA) methods are vital for the systems' objective of communicating reliable medical video to the medical expert [4], [7], [8].

In terms of wireless infrastructure, thus far, m-health video systems have been primarily based on 3G wireless networks [3], [5]. Given the limited upload data rates supported by these channels (up to 384 kb/s), the associated source encoding parameters were bounded to CIF resolution video size. As documented in [4] and [6], medical video resolution directly impacts the clinical capacity of the transmitted video. For atherosclerotic plaque ultrasound video, shifting from QCIF (176×144) to CIF (352×288) resolution enables the assessment of plaque type [6], providing critical clinical information to the medical expert for assessing the possibility of a plaque rupture, leading to stroke. Some recent studies that have briefly highlighted the benefits associated with streaming higher resolutions can be found in [4] and [9]–[11]. However, these studies are based on a limited number of cases, while the clinical aspect has not been extensively addressed. Moreover, these previous studies did not address individual network parameters' issues associated with clinical capacity of high-resolution video transmission.

As a result, there is a strong demand to investigate new 3.5G and 4G wireless technologies [12] facilitating medical video communication at the clinically acquired video resolution. Ultimately, the goal is to deliver sufficiently high resolutions and video frame rates with the low-delay and low packet loss rates (PLR) that can approach the experience of in-hospital examinations.

In this study, we investigate the added clinical value of high-resolution (4CIF-704×576) medical video communications

Manuscript received July 2, 2012; revised October 13, 2012; accepted November 27, 2012. Date of publication December 11, 2012; date of current version May 1, 2013. This work was supported by the "Diagnostically Robust Ultrasound Video Transmission over Emerging Wireless Networks," "DRIVEN" Project 301476 under the Marie Curie Actions—Intra-European Fellowships FP7-PEOPLE-2011-IEF scheme.

A. Panayides is with the Department of Electrical and Electronic Engineering, Imperial College London, London, SW7 2AZ, U.K., and also with the Department of Computer Science, University of Cyprus, Nicosia 1678, Cyprus (e-mail: a.panayides@imperial.ac.uk; panayides@ucy.ac.cy).

Z. C. Antoniou, Y. Mylonas, A. Pitsillides, and C. S. Pattichis are with the Department of Computer Science, University of Cyprus, Nicosia 1678, Cyprus (e-mail: antoniou.zinonas@ucy.ac.cy; mylonas@ucy.ac.cy; a.pitsillides@ucy.ac.cy; pattichi@ucy.ac.cy).

M. S. Pattichis is with the Department of Electrical and Computer Engineering, University of New Mexico, Albuquerque, NM 87131 USA (e-mail: pattichis@ece.unm.edu).

Color versions of one or more of the figures in this paper are available online at <http://ieeexplore.ieee.org>.

Digital Object Identifier 10.1109/TITB.2012.2232675

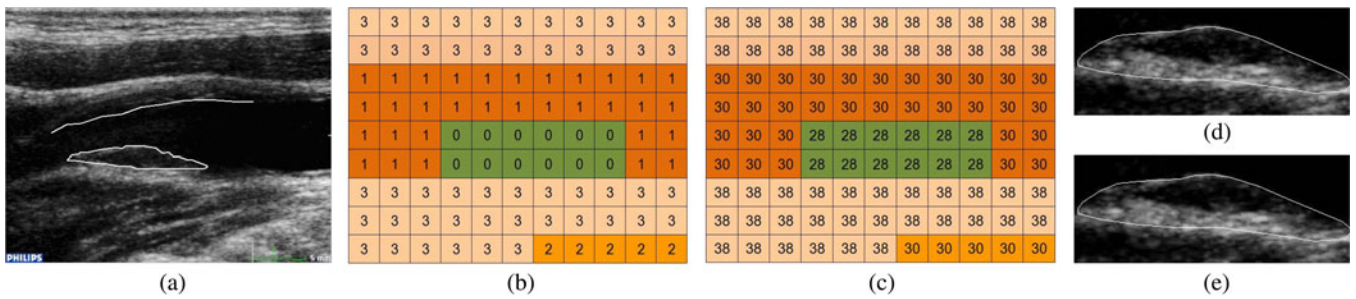


Fig. 1. Atherosclerotic plaque ultrasound variable quality slice encoding. (a) Pixel-based segmentation of diagnostically important regions (based on [13]). (b) FMO type 2 Macroblock Allocation Map (MBAmap). (c) Corresponding Quantization Parameter Allocation Map (QPAm) for variable quality slice encoding (introduced in [6]). (d) Plaque ROI segmented from original 4CIF video. (e) Plaque ROI with QP:28 segmented from 4CIF resolution video with QPs: 38/30/28.

over mobile worldwide interoperability for microwave access (WiMAX) networks for emergency telemedicine. The efficacy of the proposed end-to-end ultrasound video communication scheme is validated based on scalable clinical criteria. For this purpose, the clinically validated approach introduced [12] is extended from the CIF resolution to the higher resolution of 4CIF and the lower resolution of QCIF. In [6], diagnostically relevant selection of encoding parameters based on video region's clinical importance was used (see Fig. 1). Here, we extensively validate different medium access control (MAC) and Physical layer features of mobile WiMAX channels that can support efficient emergency telemedicine m-health systems. Most importantly, we clinically evaluate ultrasound videos transmitted using different network parameters configurations. The goal of the network study is to provide recommendations for resilient network parameter selection that will accommodate different emergency scenarios and varying network state.

We summarize the primary contributions of this paper over previously published work (see, e.g., [6]) in three different areas.

- 1) *Robust video encoding at three different resolutions:* We consider QCIF, CIF, and 4CIF resolutions and carefully discuss the clinically validated criteria associated with each spatial resolution. For each case, we measure improvement in terms of the reduction in bitrate, which can be used for increasing the peak signal-to-noise ratio (PSNR) of the reconstructed video as compared to standard H.264/AVC encoding. For this purpose, we employ the BD-PSNR algorithm, which estimates the average bitrate gains for equivalent PSNR levels for a total of 240 cases of QCIF, CIF, and 4CIF resolutions. Beyond the cases considered in [6], we consider an additional 1500 4CIF transmission cases over Mobile WiMAX.
- 2) *Relationship between spatial resolution (QCIF, CIF, 4CIF) and clinical diagnosis:* We summarize the clinical criteria that can be addressed at different resolutions (see Section IV-C). This relationship is validated through separate evaluation of the different criteria. For example, the use of 4CIF ( $704 \times 576$ ) resolution allows the use of new clinical criteria that are closer to standards used for in-hospital exams. For the current application, the additional resolution allows us to visualize atherosclerotic plaque morphology, not just the plaque type.

- 3) *Medical video communications over Mobile WiMAX networks:* We propose an emulation framework for mobile WiMAX medical video communication based on OPNET modeler. For this purpose, real ultrasound video encodings are used to generate video trace files imported to OPNET to model wireless video transmission. Following transmission, the communicated video packets are mapped back to the original files for decoding. The latter method allows us to realistically measure the effect of each investigated configuration setting both objectively and most importantly, subjectively (clinical evaluation).

Based on the previously described method, we provide recommendations for mobile WiMAX network parameter utilization for maximizing the communicated video's clinical capacity. Typical emergency telemedicine scenarios are constructed as a function of three different channel modulation and coding schemes, hybrid signal attenuation model, various distances from the base station (BS), and diverse mobility patterns. Mobile WiMAX network's performance is validated using quality of service (QoS) measurements such as PLR, packet delay, and PSNR of reconstructed video bitstreams, for an overwhelming number of 1500 video cases.

The rest of this paper is organized as follows: Section II provides a brief overview of mobile WiMAX networks and outlines their characteristics that relate to video transmission. Section III describes the undertaken methodology, while Section IV provides the experimental evaluation. Finally, Section V gives some concluding remarks.

## II. MOBILE WiMAX FOR VIDEO COMMUNICATIONS

WiMAX was first standardized for fixed wireless applications in 2004 by the IEEE 802.16-2004 and then for mobile applications in 2005 by the IEEE 802.16e standard [14]. The current WiMAX standard 802.16m, also termed as IEEE WirelessMAN-Advanced, met the ITU-R IMT-advanced requirements and is considered to be a 4G technology. In what follows, we describe the WiMAX features provided at the physical layer (PHY) and the MAC layer.

### A. Physical Layer Features

The primary features of the physical layer include adaptive modulation and coding (QPSK, 16-QAM, 64-QAM), hybrid

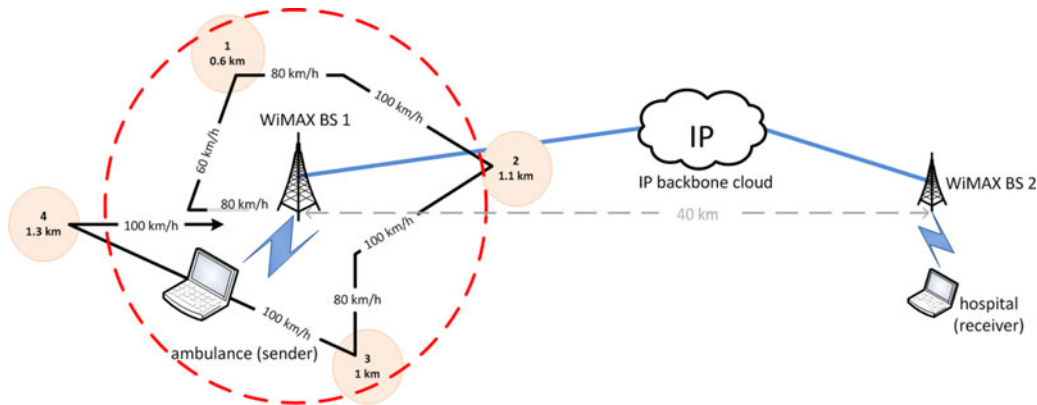


Fig. 2. Typical topology for simulating medical video transmission over mobile WiMAX networks. The ambulance travels with speeds ranging from 60 to 100 km/h following the course delineated by the black line. Vertices “1”–“4” depict the locations close to the BSs effective coverage zone used during Scenario 2.

automatic repeat request (HARQ), and fast channel feedback. WiMAX uses scalable orthogonal frequency division multiple access that divides the transmission bandwidth into multiple subcarriers. The number of subcarriers ranges from 128 for 1.25 MHz channel bandwidth and extends up to 2048 for 20-MHz channels. In this manner, dynamic QoS can be tailored to an individual application’s requirements. In addition, orthogonality among subcarriers allows overlapping leading to flat fading. In other words, multipath interference is addressed by employing OFDM, while available bandwidth can be split and assigned to several requested parallel applications for improved system’s efficiency. The latter is true for both downlink (DL) and uplink (UL). A multiple-input multiple-output antenna system improves communication performance, including significant increases in data throughput and link range, without additional bandwidth or increased transmit power.

### B. MAC Layer Features

The most important features of the MAC layer include QoS provision through different prioritization classes, direct scheduling for DL and UL, efficient mobility management, and security. The five QoS categories are described in [14] and [15]. Based on each application’s requirements, we have an appropriate QoS class with its corresponding UL burst and data rate. For real-time video streaming, the best option is to use the real-time polling service (rtPS) QoS class. The rtPS class specifies the minimum sustained data rate, the maximum traffic burst, the maximum tolerated latency, and a traffic priority, which the WiMAX air interface scheduler is designed to accommodate [15].

Mobility management is well addressed in 802.16e and current 802.16m standards, which was an issue in 802.16d primary standard for fixed connections. With a theoretical support of serving users at 120 km/h in 802.16e, established connections provide adequate performance for vehicles moving with speeds between 50 and 100 km/h.

## III. METHODOLOGY

We investigate high-resolution medical video communication performance over mobile WiMAX networks based on realistic clinical scenarios. The aim is to model realistic scenarios that can

be used to evaluate the challenges associated with developing m-health video systems for emergency telemedicine. Such a system is illustrated in Fig. 2. The key concept is to communicate the patient’s video (trauma or ultrasound) to the hospital premises, for remote diagnosis and assistance with in-ambulance care, moreover for better triage and hospital admission related tasks (e.g., surgery chamber preparation).

For the scenario depicted in Fig. 2, the medical ultrasound video transmission is launched once the paramedics have stabilized the patient, utilizing equipment residing in the ambulance. The simulated scenario models a typical route from the emergency incident to the hospital premises and highlights the technological challenges associated with the wireless communication of ultrasound video of adequate diagnostic quality.

In what follows, we provide more detailed descriptions of each block component of the proposed medical video communication framework in the context of the scenario depicted in Fig. 2.

### A. Preprocessing

This step typically involves video resolution and frame rate adjustments to match the available channel bandwidth (upload data rate) and end-user device capabilities. In this study, high-bandwidth mobile WiMAX networks allow the investigation of the transmission of 4CIF video resolution at 15 frames/s.

### B. Diagnostically Relevant Encoding

The proposed system uses a diagnostically relevant (m-aware) and resilient encoding scheme that has been described in [4] and [6]. The key idea is to associate video ROIs with clinical criteria. Each video slice is then assigned a quality level based on its diagnostic significance. These quality levels are implemented by adjusting the values of the quantization parameter as demonstrated in Fig. 1. In this manner, significant bitrate requirements can be preserved by compressing the background (nondiagnostically important region). The basic ROI approach can be extended to different medical imaging modalities and is already gaining ground in the literature [3], [4], [9].

For atherosclerotic plaque ultrasound videos, the correspondence between the ROIs and the clinical significance are as follows (see Fig. 1).

TABLE I  
TOTAL NUMBER OF PROCESSED VIDEOS IN THIS STUDY

		Diagnostically Relevant Encoding		Mobile WiMAX Transmission	
		Instances	Cases	Instances	Cases
Resolution		QCIF, CIF, 4CIF	×3	4CIF	×1
Method		FMO, FMO ROI RS	×2	FMO ROI RS	×1
QP	FMO	36/36/36, 32/32/32, 28/28/28, 24/24/24	×4	N/A	×1
	FMO ROI RS	42/38/36, 40/34/32, 38/30/28, 36/26/24		38/30/28 <sup>a</sup>	
Data Set		10 ultrasound videos	×10	10 ultrasound videos	×10
Modulation & Coding		N/A	N/A	QPSK $\frac{1}{2}$ , 16-QAM $\frac{3}{4}$ , 64-QAM $\frac{3}{4}$	×3
Video Streaming Location		N/A	N/A	Scenario 1 (video looped over entire route)	×1
				Scenario 2 (0.6 km, 1.1 km, 1 km, 1.3 km)	×4
OPNET		N/A	N/A	10 simulations runs	×10
Total number of processed videos			240	Scenario 1	300
				Scenario 2	1200

We use FMO and FMO ROI RS for constant QP FMO encoding and variable QP FMO with RS respectively.

<sup>a</sup>38:background/ 30:wall ROI/ 28:plaque ROI.

- 1) *Plaque region for visualizing plaque type, morphology, and motion*: This is the primary ROI. By visualizing the plaque type and morphology, we can assess the stability of the plaque (e.g., darker plaques turn to be more dangerous). Plaque motion patterns can also help in assessing plaque stability. The use of 4CIF resolution over WiMAX networks is particularly critical for this region (see Fig. 1 and Table VI).
- 2) *Surrounding plaque region for visualizing stenosis*: A high degree of stenosis is used as a strong predictor of the risk of stroke.
- 3) *Near and far wall regions for visualizing wall motion*: The interest in visualizing the near and far walls comes from the need to compare motion patterns with the plaque. Unstable plaques can have different motion patterns than the whole plaque.
- 4) *ECG region for visualizing ECG waveform*: The ECG is used to help visualize plaque and stenosis changes through different parts of the cardiac cycle (e.g., during systole and diastole).

In this study, we consider three different video resolutions, namely QCIF (176×144), CIF (352×288), and 4CIF (704×576), for the encoding setup depicted in the left column of Table I. The objective is to include scalable screen resolutions that are widely used in the literature today, in addition to investigating high-resolution encodings over mobile WiMAX networks. In the latter case, only 4CIF resolution with the recommended diagnostically acceptable QPs setting of 38/30/28 (see also [6]) is used.

A series of ten videos encoded at 15 frames/s is used to evaluate the proposed concept. H.264/AVC error resilient tool, flexible macroblock ordering (FMO) type 2, is used to implement variable quality slice encoding. Baseline profile, universal variable length coding entropy coding, IPPP encoding structure, with an Intra update frame interval of 15 frames, and a total of 100 frames per video summarize the encoding parameters. The JM H.264/AVC reference software [16] has been used for encoding. For the mobile WiMAX video transmission experiments, the obtained results are averaged over ten simulations runs for each scenario. Redundant slices (RS) at the encoder (one every

four coded frames) and simple frame copy error concealment at the decoder are used to recover from packet losses.

### C. Mobile WiMAX Video Transmission

We investigate high-resolution video communication performance based on the scenario illustrated in Fig. 2. Our aim is to realistically model the varying state of wireless channels that contributes to ultrasound video degradation when transmitting from the ambulance to the hospital. For this typical scenario, we investigate the use of different channel modulation and coding schemes, signal attenuation due to different signal propagation models, mobility, distance from the BS, bandwidth availability through subcarriers scalability, and QoS prioritization classes.

A synopsis of the parameters associated with the scenario of Fig. 2 appears in Table II, while the total number of processed videos is illustrated in the right column of Table I. The ambulance travels with speeds ranging from 60 to 100 km/h and traverses through locations situated near the effective coverage zone of the BS (distance range: 150 m–1.3 km). The multipath channel model is set to ITU Vehicular A, while a vehicular path loss model is also considered; with a shadow fading correction of 12 dBs (OPNET [17] implements differently path loss and multipath fading, and allows shadow fading correction for increasing possible signal attenuation combinations during simulations). Three different channel modulation and coding schemes are investigated, namely QPSK  $\frac{1}{2}$ , 16-QAM  $\frac{3}{4}$ , and 64-QAM  $\frac{3}{4}$ , with the number of subcarriers set to 512, besides QPSK  $\frac{1}{2}$  which is set to 2014.

1) *Scenario 1*: For a more realistic evaluation, the ultrasound video traffic sent through the network is modeled via trace files generated using real ultrasound video encodings. In *Scenario 1*, the ultrasound videos are looped over the entire route to examine the wireless channel's performance by measuring the average QoS parameters such as PLR, end-to-end delay, and delay jitter.

2) *Scenario 2*: In *Scenario 2*, ultrasound video traffic is initiated at four different locations (see Fig. 2) selected to highlight the wireless channel's ability to provide reliable medical video communications at different distances from the BS. Following the wireless transmission and the QoS measurements, the

TABLE II  
MOBILE WiMAX NETWORK CONFIGURATION PARAMETERS

Parameter	Value	Parameter	Value
Access Technology	OFDMA 20MHz	Frame Duration	5ms
Base Frequency	5.8 GHz	Symbol Duration	100.8
Subcarrier Frequency Spacing	10.9375 KHz	Total Capacity DL/UL	2.88 / 0.576 Msps (512 subcarriers) <sup>1</sup> 9.216 / 2.6112 Msps (2048 subcarriers) <sup>2</sup>
ARQ/hARQ	Disabled	Duplexing Technique	TDD
Number Transmit/ Receive Antennas	BS: 1, MS: 1	Multipath Channel Model/ Pathloss Model/ Shadow Fading	ITU Vehicular A/ Vehicular Environment/ 12 dB
Antenna Gain	BS: 15 dBi, MS: -1dBi	Additive Correction in dBs	
Maximum Transmission Power	BS: 2 W, MS: 0.5W	MAC Layer QoS Class	Real time polling service (rtps)
Modulation and Coding	QPSK $\frac{1}{2}$ , 16-QAM $\frac{3}{4}$ , 64-QAM $\frac{3}{4}$	Minimum Sustained Data Rate <sup>3</sup>	768 kbps, 1 Mbps, 1.3 Mbps, 1.5 Mbps
		Mobility	60-100 Km/h

OFDMA: Orthogonal Frequency Division Multiple Access, TDD: Time Division Duplexing, ARQ: Automatic Repeat reQuest, hARQ: Hybrid Automatic Repeat request, DL: Downlink, UL: Uplink, Msps: Mega Symbols per Second, BS: Base Station, MS: Mobile Station.

<sup>1</sup>16-QAM  $\frac{3}{4}$ : 3/b/symbol/Hz \* Msps (512 subcarriers) = 8.64/ 1.728 Mbps, 64-QAM  $\frac{3}{4}$ : 4.5 b/symbol/Hz \* Msps (512 subcarriers) = 12.96/ 2.592 Mbps, <sup>2</sup>QPSK  $\frac{1}{2}$ : 1 b/symbol/Hz \* Msps (2048 subcarriers) = 9.216 / 2.6112 Mbps, <sup>3</sup>For the 10 atherosclerotic plaque ultrasound videos of the dataset.

successfully streamed packets are mapped back to the original RTP files, decoded, and evaluated by the relevant medical expert. In addition to the wireless network's QoS measurements, VQA ratings described below summarize the evaluation setup.

#### D. Video Quality Assessment

VQA includes objective and subjective evaluations. Objective VQA is given in terms of the video quality metric (e.g., PSNR) computed over the specified video slices using the clinical criteria. Clinical evaluation is performed by the relevant medical expert for the clinical criteria provided in Table VI. Ratings are given in the range of 1–5. A rating of 5 is the highest possible and it signifies that the diagnostic information in the decoded video is of essentially the same quality as the original video. A rating of 4 indicates that there is a diagnostically acceptable loss of minor details. At the lowest scale, a rating of 1 signifies that the decoded video is of unacceptably low quality.

## IV. RESULTS AND DISCUSSION

In this section, we discuss the experimental evaluation of the proposed medical ultrasound video transmission framework. We present results in terms of video encoding, medical video transmission over mobile WiMAX channels, and clinical evaluation.

#### A. Diagnostically Relevant Encoding

To demonstrate the efficiency of the proposed diagnostically relevant encoding scheme, we provide a comparative evaluation of: 1) FMO with constant QP video slices and 2) FMO with variable QPs and RS for communications in noisy environments. For each method, we had four sets of quantization levels for the video slices as depicted in Table I.

Table III depicts the associated bitrate gains of the proposed variable quality slice encoding scheme when compared to the conventional uniformly encoded medical video. Fig. 3 uses boxplots to illustrate the bitrate requirements of the medical ultrasound video dataset, for the two investigated encoding schemes. Bitrate gains for equivalent perceptual quality are computed using the BD-PSNR algorithm [18], based on the four rate points

TABLE III  
AVERAGE BIT RATE GAINS OF DIAGNOSTICALLY RELEVANT ENCODING WHILE MAINTAINING THE SAME DIAGNOSTIC QUALITY FOR FMO ROI RS VERSUS FMO<sup>1</sup>

	QCIF	CIF	4CIF
Bit Rate Gain (%)	34.7	39.8	42.3

<sup>1</sup>FMO ROI RS stands for variable quality slice encoding with redundant slices. FMO stands for standard H.264/AVC FMO type 2 encoding.

Bitrate gains account for the reductions in bitrate requirements for equivalent objective quality (PSNR), estimated using the BD-PSNR algorithm for QP values: 36, 32, 28, and 24.

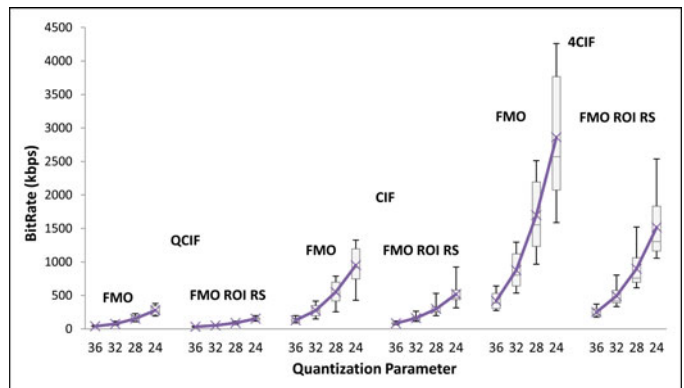


Fig. 3. Boxplots depicting bitrate requirements for equivalent perceptual quality of the two investigated encodings schemes, using four QPs and QCIF, CIF, and 4CIF video resolutions.

shown in Fig. 3. The average bitrate demands reductions are 42.3% for 4CIF, 39.8% for CIF, and 34.7% for QCIF resolution videos. Bitrate gains are functions of the area occupied by the diagnostic ROIs, and most of the savings come from compressing the background (see Fig. 1). Here, the medical video dataset comprises videos with diagnostic ROIs ranging between 44% and 72% of the entire video [4].

#### B. Mobile WiMAX Medical Video Transmission

1) *Scenario 1*: Table IV records the averaged QoS measurements of all video transmission simulations. QPSK  $\frac{1}{2}$  channel modulation scheme provides for a more robust performance as

TABLE IV  
QoS MEASUREMENTS FOR SCENARIO 1

Channel Modulation & Coding Schemes		QPSK $1/2$		16-QAM $3/4$			64-QAM $3/4$		
QoS Parameters	PLR % ( $\sigma$ ) <sup>1</sup>	Delay (ms)	Jitter (ms)	PLR % ( $\sigma$ )	Delay (ms)	Jitter (ms)	PLR % ( $\sigma$ )	Delay (ms)	Jitter (ms)
Total Avg.	1.0 (0.1)	21.38	<1	3.8 (3.85)	20.34	<1	4.38 (5.19)	20.62	<1

<sup>1</sup> $\sigma$ : standard deviation.

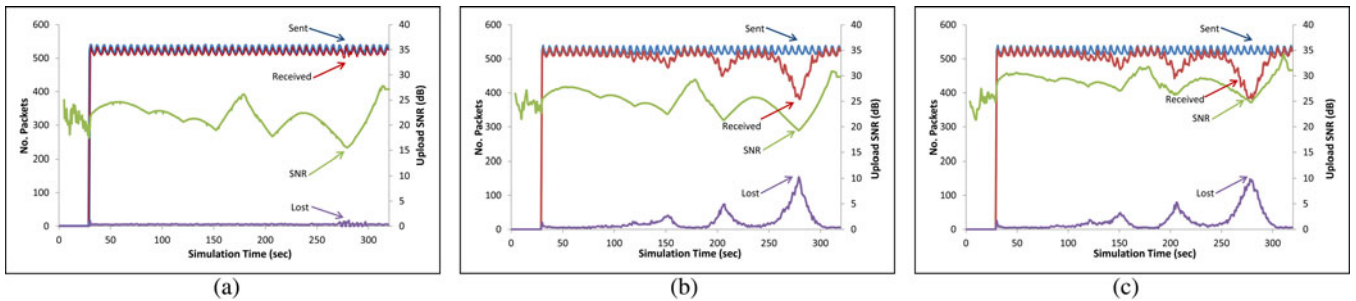


Fig. 4. Packet losses as a function of the distance from the BS (illustrated via simulation time) and SNR for the investigated channel modulation and coding schemes (for a typical video looped over the entire route of Fig. 2, video duration = 7 s, Scenario 1). (a) Packet losses for QPSK  $1/2$ . (b) Packet losses for 16-QAM  $3/4$ . (c) Packet losses for 64-QAM  $3/4$ .

the PLR measured are in the order of 1%. This is also highlighted in Fig. 4(a) for the video shown in Fig. 1(a). 16-QAM  $3/4$  and 64-QAM  $3/4$  depict comparable performance with PLR extending up to 5%. At these PLR, the reconstructed ultrasound videos still yield acceptable diagnostic performance, due to the use of RS and FMO error-resilience features. By examining the PLR standard deviation in Table IV, however, we observe that PLR for 16-QAM  $3/4$  and 64-QAM  $3/4$  vary significantly and can reach unacceptably high rates. This is more clearly visualized in Fig. 4(b) and (c), where it is obvious that significant packet losses occur at large distances to the BS. This is not the case for QPSK  $1/2$  scheme, which exhibits a robust performance throughout the simulation irrespective of the varying channel conditions. The reasoning is that QPSK  $1/2$  requires lower signal-to-noise ratio (SNR) compared to 16-QAM  $3/4$  and 64-QAM  $3/4$  [19] to maintain a quality connection. This is clearly depicted in Fig. 4, where the upload SNR (measured each second) fluctuations experienced by packets traversing from the mobile station to the BS do not result in packet losses for QPSK  $1/2$  as in the rival channel modulation and coding schemes. This benefit comes at the expense of the channel's capacity as depicted in Table II. QPSK  $1/2$  conveys information at 1 bit/symbol/Hz, as compared to 16-QAM  $3/4$  and 64-QAM  $3/4$ , which provide 3 and 4.5 bits/symbol/Hz, respectively (mobile WiMAX capacity is given at mega symbols per second—MSPs). As a result, QPSK  $1/2$  utilizes 2048 subcarriers at 20 MHz to meet the channel capacity required to transmit 4CIF resolution medical video, whereas 16-QAM  $3/4$  and 64-QAM  $3/4$  only require 512 subcarriers.

Average end-to-end delay of transmitted packets for all three channel modulations and coding schemes examined is less than 22 ms, which is well within the acceptable bounds for medical video streaming applications [19] (300 ms but preferably less than 100 ms). Similarly, delay jitter is negligible for the

presented scenario. This is partly due to the fact that in this particular scenario, no background traffic is modeled, while the RTP packets do not traverse through multiple nodes to reach their destination. However, even in the previously described circumstances, the use of service prioritization classes (as detailed in Section II) allows mobile WiMAX networks to meet the individual QoS requirements of each service.

2) *Scenario 2*: To better examine the performance of the system for transmission near the boundaries of the BS's effective coverage zone, a second scenario was implemented where the mobile station transmits only one video loop at each of the four different distances from the BS depicted in Fig. 2 (in *Scenario 1*, each video is looped until the end of each simulation). In this way, the actual quality of the transmitted video can be computed, both objectively and subjectively, as well as the specific QoS measurements at these locations, allowing accurate assumptions as to the extent (as a function of the distance from the BS and mobility) that the investigated channel modulation and coding schemes can be used.

Results are shown in Table V and Fig. 5. As expected, QPSK  $1/2$  attains diagnostically acceptable QoS measurements in all four locations, with consistently low PLR and high PSNR scores around 39 dB [see leftmost boxplots of Fig. 5(a)]. Here, we use the term *diagnostically acceptable* to refer to the fact that the attained plaque ROI PSNR values are above 35 dB that were shown to qualify for clinical practice in [6].

16-QAM  $3/4$  and 64-QAM  $3/4$  deliver diagnostically acceptable performance comparable to QPSK  $1/2$  only for the first location, which is situated closer to the BS [see location "1" in Fig. 2 and leftmost boxplots of Fig. 5(b)]. As the mobile station (ambulance) moves away from the BS and signal attenuation increases, the quality of the video can be significantly degraded. At 1 km from the BS, diagnostically acceptable average PSNR ratings are still obtained. The experienced PLR and the

TABLE V  
QoS MEASUREMENTS FOR SCENARIO 2

Channel Modulation & Coding Schemes	QPSK $\frac{1}{2}$			16-QAM $\frac{3}{4}$			64-QAM $\frac{3}{4}$		
	QoS Parameters	PLR % ( $\sigma$ ) <sup>1</sup>	Delay (ms)	PSNR <sup>2</sup> (dB)	PLR % ( $\sigma$ )	Delay (ms)	PSNR (dB)	PLR % ( $\sigma$ )	Delay (ms)
1 (0.6 km from BS)	1.42 (0.22)	20.76	39.17	1.82 (0.77)	20.04	39.01	1.68 (0.98)	20.24	39.11
3 (1 km from BS)	1.25 (0.21)	21.41	38.91	5.28 (5.67)	19.99	37.23	5.82 (7.39)	20.20	37.11
2 (1.1 km from BS)	1.24 (0.32)	22.65	38.87	6.07 (6.77)	19.95	37.34	7.22 (8.98)	20.19	36.83
4 (1.3 km from BS)	1.36 (0.50)	24.07	39.01	16.27 (17.64)	19.82	34.98	16.5 (20.47)	19.99	34.74

<sup>1</sup> $\sigma$ : standard deviation, <sup>2</sup>PSNR is given for the atherosclerotic plaque ROI extracted from the transmitted ultrasound video.

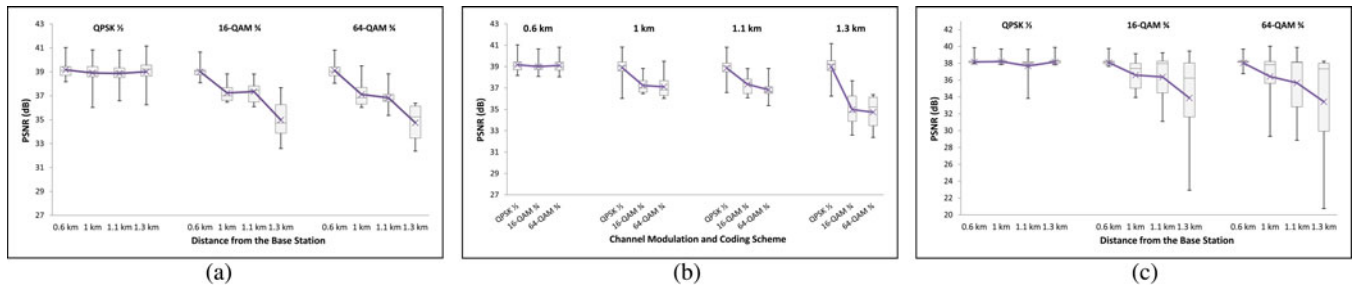


Fig. 5. Scenario 2 QoS Evaluation: (a) Boxplots depicting the average PSNR ratings for the whole dataset and for each channel modulation and coding scheme, as a function of the distance from the BS. (b) Boxplots depicting the average PSNR ratings for the whole dataset and for each distance from the BS, as a function of the investigated channel modulation and coding schemes. (c) Boxplots depicting PSNR ratings for the ten random emulations of a single video (video shown in Fig. 1 and used in Fig. 4) for each channel modulation and coding scheme, as a function of the distance from the BS.

associated PLR standard deviation, however, suggest that ultrasound video of unacceptable clinical quality is transmitted at some occasions. This is more obvious at location “2” (1.1 km from BS) and 64-QAM  $\frac{3}{4}$ , as shown in Fig. 5(c). Here, it is important to note that the depicted results in Fig. 5(a) and (b) are boxplots based on PSNR averages of ten simulation runs of the ten videos parting the ultrasound video dataset. On the other hand, Fig. 5(c) depicts boxplots reporting the PSNR ratings for each of the ten simulation runs, for the video depicted in Fig. 1(a). The latter case demonstrates the extreme channel conditions a mobile station is likely to experience when transmitting at the effective coverage zone of the BS. As shown in Fig. 5(c), increased number of packet losses and high PLR standard deviation, as already discussed above, often results in diagnostically unacceptable PSNR ratings.

The latter observation is verified during the clinical evaluation (see clinical evaluation section below) where different video instances are clinically validated. At the furthest location, high PLR make the transmitted video of limited clinical interest. Consequently, distances greater than 1 km from the BS provide for a boundary case for this scenario.

The results from the objective evaluation significantly extend the findings of previous studies in the literature [4], [9]–[11]. Here, additional experimentation allowed investigating higher mobile speeds up to 100 km/h (compared to 50 km/h [4], [9]), distances between 150 m and 1.3 km from the BS (compared to 500 m [4], [9]), hybrid vehicular multipath and path loss propagation models (compared to free space [10], [11] and vehicular models [9]), and subcarriers scalability up to 2048 (compared to 512 [9] and 1024 [4]), for a dataset composed of ten ultrasound videos and an overwhelming number of investigated cases. Most importantly, the clinical capacity of the communi-

TABLE VI  
RELATIONSHIP BETWEEN CLINICAL CRITERIA AND VIDEO RESOLUTION

	QCIF	CIF	4CIF
<i>Plaque Detection</i>	√	√	√
<i>Artery Stenosis</i>	√	√	√
<i>Plaque Type</i>		√	√
<i>Plaque Morphology</i>			√

TABLE VII  
CLINICAL EVALUATION FOR THE INVESTIGATED CHANNEL MODULATION AND CODING SCHEMES AS A FUNCTION OF THE DISTANCE FROM THE BS

Resolution: 4CIF, Frame Rate: 15fps, QP: 38/30/28 <sup>a</sup> , BitRate: 1.5 Mbps			
Location <sup>b</sup>	QPSK $\frac{1}{2}$	16-QAM $\frac{3}{4}$	64-QAM $\frac{3}{4}$
<i>Plaque Detection</i>	5/ 5/ 5/ 5	5/4.3/4.5/3.4	5/ 4.2/ 4.4/3.6
<i>Artery Stenosis</i>	5/ 5/ 5/ 5	5/4.1/4.2/3.4	5/ 4/ 4.3/3.6
<i>Plaque Type</i>	5/ 5/ 5/ 5	5/4.1/4.2/3.3	5/ 4/ 4.3/3.5
<i>Plaque Morphology</i>	5/ 5/ 5/ 5	5/4.1/4.2/3.3	5/ 4/ 4.3/3.5

1: Lowest Score, 5: Highest Score

<sup>a</sup>QP are given in the order of background/wall ROI/plaque ROI, i.e. 38:background/ 30:wall ROI/ 28:plaque ROI.

<sup>b</sup>Distance from the BS: 1: 0.6 km, 2: 1.1 km, 3: 1 km, 4: 1.3 km.

cated ultrasound videos was supported by the clinical evaluation provided below.

### C. Clinical Evaluation

1) *High-Resolution Encoding*: Table VI depicts the added clinical value linked with higher resolution medical video communication. A total of ten videos were displayed at both

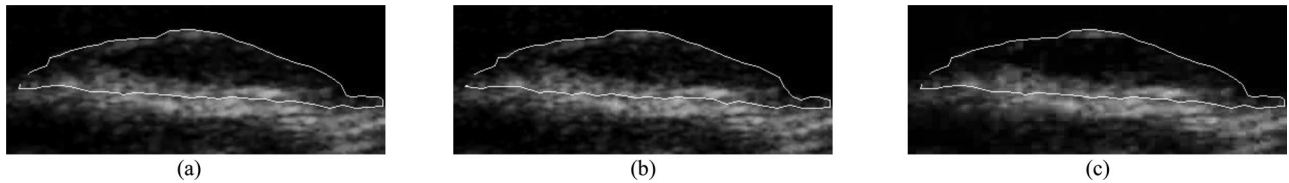


Fig. 6. Video image examples of Scenario 2 (pixel segmentation based on [13]). (a) Plaque ROI PSNR: 38.2 dB, channel modulation & coding: QPSK  $^{1/2}$ , distance from BS: 1.3 km. (b) Plaque ROI PSNR: 37.36 dB, channel modulation & coding: 16-QAM  $^{3/4}$ , distance from BS: 1.1 km. (c) Plaque ROI PSNR: 29.34 dB, channel modulation & coding: 16-QAM  $^{3/4}$ , distance from BS: 1.3 km.

CIF and 4CIF resolutions. The medical expert was asked to comment on the clinical content of these two resolutions. Based on previous knowledge, CIF resolution provided for evaluating the clinical criterion of plaque type, something which was not feasible with lower QCIF resolution. The findings verified the hypothesis that higher resolution is associated with communicating a larger amount of clinical information. Detailed assessment of plaque morphology is made possible for 4CIF resolution medical video. This was not always the case with lower CIF resolution.

However, the key finding in these experiments is that 4CIF resolution closely matches the clinical capacity of the original video. Similar to [7] and [8], the medical expert was also asked to rate whether the encoded video contained the same amount of clinical information as the original video. The medical expert concluded that the clinical information precision found in 4CIF resolution ultrasound video is comparable to that of the ultrasound device's monitor. It is associated with better assessment of the plaque motion and plaque components movement, which leads to confident assessment of plaque type and plaque morphology, aligned with diagnosing possibility of plaque rupture. Moreover, it facilitates better visualization of the intima of the near and far walls, of the plaque components, and the fibrous cap where this is applicable. In general, it is expected to reduce interobserver variability. On the other hand, a higher frame rate than 15 frames/s may be required to rival in-hospital examination.

2) *Scenario 2*: Table VII summarizes the clinical evaluation of investigated locations of the previously described *Scenario 2*. It evaluates the capability of mobile WiMAX networks to communicate high-resolution medical ultrasound video. Here, we present mean opinion scores of a representative sample of the 120 instances (3 channel modulation and coding schemes  $\times$  4 locations  $\times$  10 simulation runs = 120 instances) of the video shown in Fig. 1(a).

Videos decoded after transmission using QPSK  $^{1/2}$  attain the highest clinical ratings. This is aligned with the objective assessment depicted in Table V, and the associated high PSNR scores. 16-QAM  $^{3/4}$  and 64-QAM  $^{3/4}$  attain diagnostically acceptable ratings (marginal at 1.1 km from the BS) in all but the most distant (last) location, where they fail to qualify for clinical practice. Clearly, when the distance from the BS exceeds 1 km, a switch to a more robust channel modulation scheme will prevent clinical quality to fall below of what is acceptable. Fig. 6 depicts video image examples of the investigated schemes. The artifacts in Fig. 6(c) demonstrate the limits in trying to visualize plaque

morphology at this larger distance. Even at 4CIF resolution, the plaque morphology cannot be visualized with 16-QAM  $^{3/4}$  at a distance of 1.3 km.

## V. CONCLUDING REMARKS

This paper proposes an H.264/AVC-based framework for the wireless transmission of atherosclerotic plaque ultrasound video over mobile WiMAX networks. The depicted diagnostically driven encoding scheme shows that equivalent clinical quality can be obtained at significantly reduced bitrate demands. When combined with recent postprocessing error concealment techniques [11], it can provide for additional diagnostic resilience. Comprehensive experimentation showed that low-delay high-resolution 4CIF ultrasound video transmission is possible over mobile WiMAX networks, even at speeds of 100 km/h and distances of 1 km from the BS. The investigated channel modulation and coding schemes verified that QPSK  $^{1/2}$  is the most robust scheme, especially when transmitting from locations with low SNR. On the other hand, 16-QAM  $^{3/4}$  and 64-QAM  $^{3/4}$  provide higher network capacities and are preferable when the transmitting station is closer to the BS. The performance of the system in terms of transmitted video's quality was evaluated using both objective and subjective evaluations. Clinical validation verified the capacity of mobile WiMAX networks to provide robust, clinically acceptable 4CIF ultrasound video transmission, thus enabling the transmission of ultrasound video at resolutions close to the original's video acquired resolution.

Ongoing research includes video transmission simulations over long-term evolution (LTE) and LTE-Advanced wireless channels using OPNET network simulator, as well as real-time setups. In the future, we also want to investigate how diagnostic encoding based on the emerging high efficiency video coding (HEVC) standard [20] can lead to more efficient, error-resilient encoding [21]. Moreover, the proposed framework is currently validated for use in other medical video modalities.

## ACKNOWLEDGMENT

The authors would like to thank Dr. M. Pantziaris of the Cyprus Institute of Neurology and Genetics for valuable discussions on the diagnostic issues related to atherosclerotic plaque ultrasound video, and for providing the clinical evaluation for this study.

## REFERENCES

- [1] C. S. Pattichis, E. Kyriacou, S. Voskarides, M. S. Pattichis, and R. Istepanian, "Wireless telemedicine systems: An overview," *IEEE Antennas Propag. Mag.*, vol. 44, no. 2, pp. 143–153, Apr. 2002.
- [2] E. Kyriacou, M. S. Pattichis, C. S. Pattichis, A. Panayides, and A. Pitsillides, "m-Health e-Emergency systems: Current status and future directions," *IEEE Antennas Propag. Mag.*, vol. 49, no. 1, pp. 216–231, Feb. 2007.
- [3] A. Panayides, M. S. Pattichis, C. S. Pattichis, and A. Pitsillides, "A tutorial for emerging wireless medical video transmission systems [Wireless Corner]," *IEEE Antennas Propag. Mag.*, vol. 53, no. 2, pp. 202–213, Apr. 2011.
- [4] A. S. Panayides, "Diagnostically resilient encoding, wireless transmission, and quality assessment of medical video," Ph.D. Dissertation, Dept. Comput. Sci., Univ. Cyprus, Nicosia, Cyprus, 2011.
- [5] A. Panayides, M. S. Pattichis, C. S. Pattichis, C. N. Schizas, A. Spanias, and E. C. Kyriacou, "An overview of recent end-to-end wireless medical video telemedicine systems using 3G," in *Proc. Annu. Int. Conf. IEEE Eng. Med. Biol. Soc.*, Buenos Aires, Argentina, Aug. 31–Sep. 4, 2010, pp. 1045–1048.
- [6] A. Panayides, M. S. Pattichis, C. S. Pattichis, C. P. Loizou, M. Pantziaris, and A. Pitsillides, "Atherosclerotic plaque ultrasound video encoding, wireless transmission, and quality assessment using H.264," *IEEE Trans. Inf. Technol. Biomed.*, vol. 15, no. 3, pp. 387–397, May 2011.
- [7] A. Alesanco, C. Hernandez, A. Portoles, L. Ramos, C. Aured, M. Garcia, P. Serrano, and J. Garcia1, "A clinical distortion index for compressed echocardiogram evaluation: recommendations for Xvid codec," *Physiol. Meas.*, vol. 30, no. 5, pp. 429–440, 2009.
- [8] E. Cavero, A. Alesanco, and J. Garcia, "Enhanced protocol for real time transmission of echocardiograms over wireless channels," *IEEE Trans. Biomed. Eng.*, vol. 59, no. 11, pp. 3212–3220, Nov. 2012.
- [9] M. G. Martini and C. T. E. R. Hewage, "Flexible macroblock ordering for context-aware ultrasound video transmission over mobile WiMAX," *Int. J. Telem. Appl.*, vol. 2010, p. 14, 2010.
- [10] A. Alinejad, N. Philip, and R. Istepanian, "Cross layer ultrasound video streaming over mobile WiMAX and HSPA networks," *IEEE Trans. Inf. Technol. Biomed.*, vol. 16, no. 1, pp. 31–39, Jan. 2012.
- [11] C. Debono, B. Micallef, N. Philip, A. Alinejad, R. Istepanian, and N. Amso, "Cross layer design for optimised region of interest of ultrasound video data over mobile WiMAX," *IEEE Trans. Inf. Technol. Biomed.*, vol. 16, no. 6, pp. 1007–1014, Nov. 2012.
- [12] Rysavy Research, LLC (2010). Transition to 4G, 3GPP broadband evolution to IMT-Advanced. [Online]. Available: <http://www.4gamericas.org/>
- [13] C. P. Loizou, C. S. Pattichis, M. Pantziaris, and A. Nicolaidis, "An integrated system for the segmentation of atherosclerotic carotid plaque," *IEEE Trans. Inf. Technol. Biomed.*, vol. 11, no. 5, pp. 661–667, Nov. 2007.
- [14] *IEEE Standard for Local and metropolitan area networks Part 16: Air Interface for Fixed and Mobile Broadband Wireless Access Systems, Amendment 2: Physical and Medium Access Control Layers for Combined Fixed and Mobile Operation in Licensed Bands*, IEEE Std. 802.16e-2005, and IEEE Std. 802.16-2004/Cor1-2005, Corrigendum 1, Dec. 2005.
- [15] M. Alasti, B. Neekzad, C. Jie Hui, and R. Vannithamby, "Quality of service in WiMAX and LTE networks [Topics in Wireless Communications]," *IEEE Commun. Mag.*, vol. 48, no. 5, pp. 104–111, May 2010.
- [16] H.264/AVC JM Reference Software. (Mar. 2013). [Online]. Available: <http://iphome.hhi.de/suehring/tml/>
- [17] OPNET University Program. (Mar. 2013). [Online]. Available: <http://www.opnet.com/services/university/>
- [18] G. Bjøntegaard, "Improvements of the BD-PSNR model," ITU-T SG16 Q.6 Document, VCEG-A111, Berlin, Germany, Jul. 2008.
- [19] D. Niyato, E. Hossain, and J. Diamond, "IEEE 802.16/WiMAX-based broadband wireless access and its application for telemedicine/e-health services," *IEEE Wireless Commun.*, vol. 14, no. 1, pp. 72–83, Feb. 2007.
- [20] G. J. Sullivan, J.-R. Ohm, W.-J. Han, and T. Wiegand, "Overview of the high efficiency video coding (HEVC) standard," *IEEE Trans. Circuits Syst. Video Technol.*, vol. 22, no. 12, pp. 1649–1668, Dec. 2012.
- [21] A. Panayides, Z. Antoniou, M. S. Pattichis, C. S. Pattichis, and A. G. Constantinides, "High efficiency video coding for ultrasound video communication in M-health systems," in *Proc. Annu. Int. Conf. IEEE Eng. Med. Biol. Soc.*, San Diego, CA, USA, Aug. 28–Sep. 1, 2012, pp. 2170–2173.



**Andreas Panayides** received the B.Sc. degree from the Department of Informatics and Telecommunications, National and Kapodistrian University of Athens, Athens, Greece, in 2004, the M.Sc. degree in computing and internet systems from Kings College London, London, U.K., in 2005, and the Ph.D. degree from the University of Cyprus, Nicosia, Cyprus, in 2011.

He is currently a Marie Curie Research Fellow in the Communication and Signal Processing Group, Department of Electrical and Electronic Engineering, Imperial College London. His research interests include medical video processing and communications, eHealth applications, and mobile telecommunication networks. He has published four journal publications, 15 conference papers, and two chapters in books in these areas. His research funding comes from the project Diagnostically Robust Ultrasound Video Transmission over Emerging Wireless Networks, 301476, FP7-PEOPLE-2011-IEF scheme.



**Zinonas C. Antoniou** was born in Nicosia, Cyprus, in 1984. He received the Diploma degree from the School of Electrical and Computer Engineering, National Technical University of Athens, Athens, Greece, in 2010. He is currently working toward the Ph.D. degree in the Department of Computer Science, University of Cyprus, Nicosia, Cyprus, under the guidance of Prof. C. Pattichis, and is a member of the eHealth Laboratory.

His major research interests include video processing and communications and mobile telecommunication networks. He has been a member of an IEEE society since 2012.



**Yiannos Mylonas** received the B.Sc. degree in computer engineering from Oregon State University, Corvallis, USA, in 1998. In 2001, he completed his graduate studies and received the M.Sc. degree in computer science from the University of Cyprus, Nicosia, Cyprus, where he also received the Ph.D. degree in vehicular ad hoc networks in 2010.

He was with Intel Corporation as a Product Support Engineer. Since 2001, he has been working as a Special Teaching Staff in the Department of Computer Science of University of Cyprus. The title of his research is "Speed Adaptive Probabilistic Flooding for Vehicular Ad-hoc Networks."



**Marios S. Pattichis** (M'99–SM'06) received the B.Sc. degree (high honors and special honors) in computer sciences and the B.A. degree (high honors) in mathematics in 1991, the M.S. degree in electrical engineering in 1993, and the Ph.D. degree in computer engineering from the University of Texas at Austin, Austin, USA, in 1998.

He is currently a full Professor in the Department of Electrical and Computer Engineering (ECE), University of New Mexico (UNM), Albuquerque, NM, USA, where he is also serving as a Program Chair of the Computer Engineering program. His current research interests include mathematical models for digital image, video processing and communications, dynamically reconfigurable computer architectures, and applications in biomedical and space imaging.

Dr. Pattichis is an Associate Editor of the IEEE Transactions on Image Processing. He was the General Chair of the 2008 IEEE Southwest Symposium on Image Analysis and Interpretation. At UNM, he received the 2004 ECE Distinguished Teaching Award and the 2006 School of Engineering Harrison Faculty Recognition Award.



**Andreas Pitsillides** received the B.Sc. degree from the Department of Electrical and Electronic Engineering, University of Manchester Institute of Science and Technology (UMIST), Manchester, U.K., in 1980, and the Ph.D. degree from the Swinburne University of Technology, Melbourne, Australia, in 1993.

Currently, he is a Professor with the Department of Computer Science, University of Cyprus, Nicosia, Cyprus, and heads NetRL, the Networks Research Laboratory. He has a particular interest in adapting tools from various fields of applied mathematics such as control theory, nature inspired techniques, and computational intelligence to solve problems in computer networks. He has published more than 230 referred journal papers in flagship IEEE, Elsevier, IFAC, Springer journals, international conferences and book chapters, two books (one edited), participated in over 30 European Commission and locally funded research projects with over 4.5 million Euro as principal or co-principal investigator, presented keynotes, invited lectures at major research organizations, short courses at international conferences and short courses to industry, and serves/served on several journal and conference executive committees. His research interests include fixed and mobile/wireless networks, the Internet of Things and Web of Things, and Internet technologies and their application in Mobile e-Services.



**Constantinos S. Pattichis** received his diploma as technician engineer from the Higher Technical Institute, Cyprus, in 1979, the B.Sc. degree in electrical engineering from the University of New Brunswick, Canada, in 1983, the M.Sc. degree in biomedical engineering from the University of Texas at Austin, USA, in 1984, the M.Sc. degree in neurology from the University of Newcastle Upon Tyne, U.K., in 1991, and the Ph.D. degree in electronic engineering from the University of London, U.K., in 1992.

He is currently a Professor with the Department of Computer Science and Director of the eHealth Lab of the University of Cyprus, Nicosia, Cyprus. He has a 20-year experience in eHealth systems, medical imaging, biosignal analysis, intelligent systems, and more recently in life sciences informatics. He has been involved in numerous projects in these areas funded by EU and other bodies, with a total funding managed close to 7 million Euro. He has published 74 journal publications, 182 conference papers, and 27 chapters in books in these areas. He is a Co-Editor of the books *M-Health: Emerging Mobile Health Systems*, and *Ultrasound and Carotid Bifurcation Atherosclerosis*, published in 2006 and 2012 by Springer.

Prof. Pattichis was a Guest Co-Editor of the Special Issues of the IEEE TRANSACTIONS ON INFORMATION TECHNOLOGY IN BIOMEDICINE on Emerging Technologies in Biomedicine, Computational Intelligence in Medical Systems, Citizen Centered e-Health Systems in a Global Health-care Environment, and Atherosclerotic Cardiovascular Health Informatics. He was the General Chair of the IEEE 12th International Conference on BioInformatics and BioEngineering, and 9th International Conference on Information Technology Applications in Biomedicine.